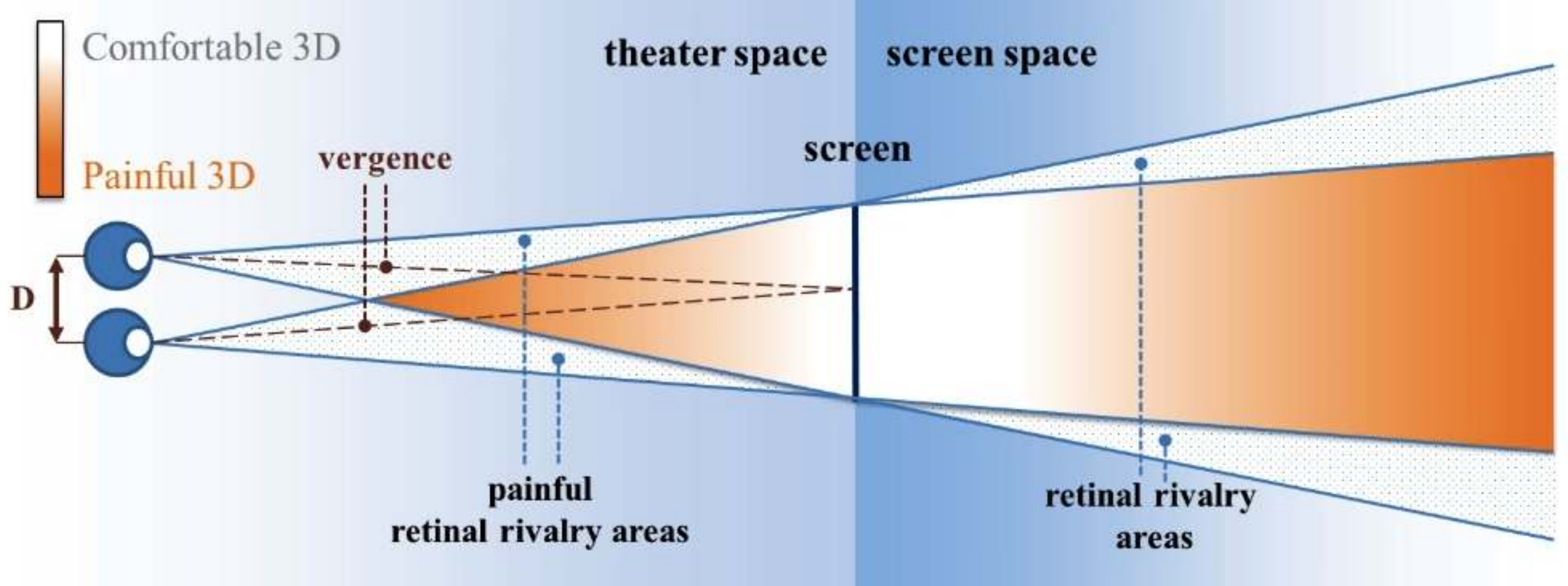


Nonlinear Disparity Mapping for Stereoscopic 3D

Manuel Lang, Alexander Hornung, Oliver Wang, Steven
Poulakos, Aljoscha Smolic, Markus Gross

Presenter: Yeon Jin (Grace) Lee
Discussant: Robin Gaestral

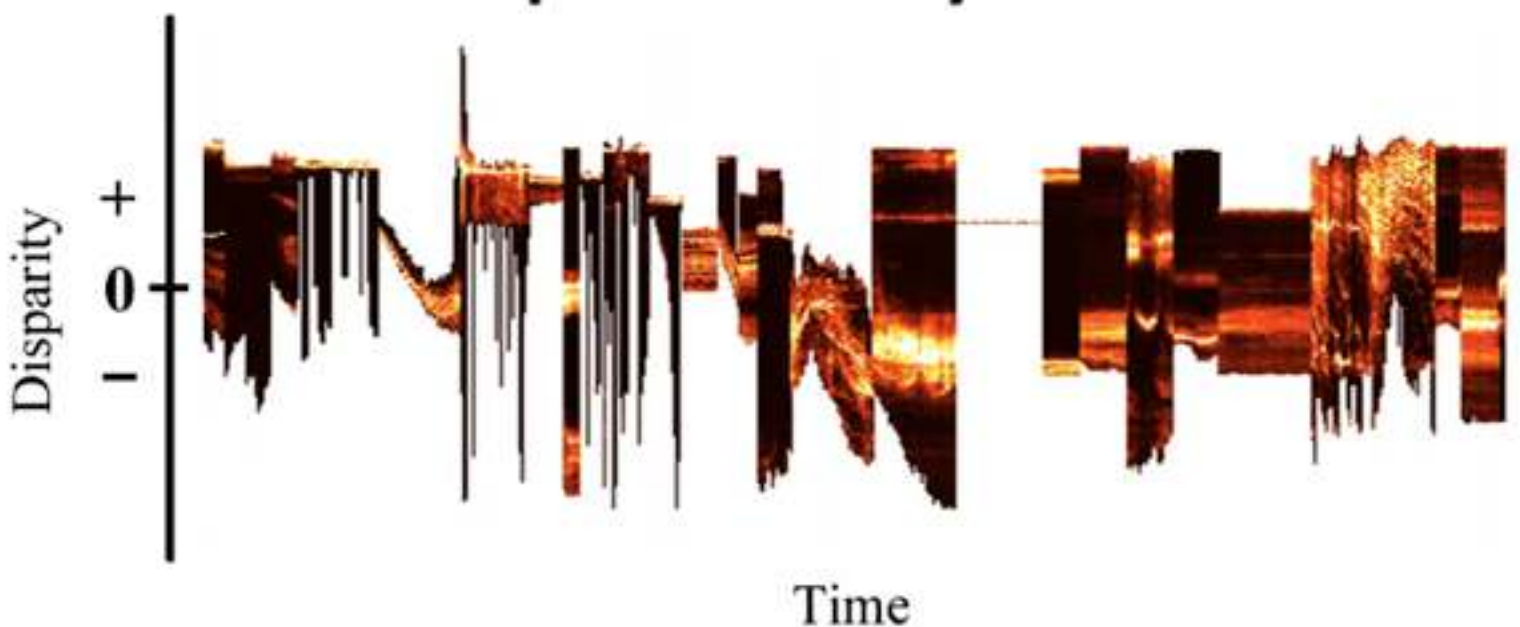
Motivation



Slide courtesy of Lang et al.

stereographer has to
carefully plan a
3D production

depth storyboard



Slide courtesy of Lang et al.

Contributions

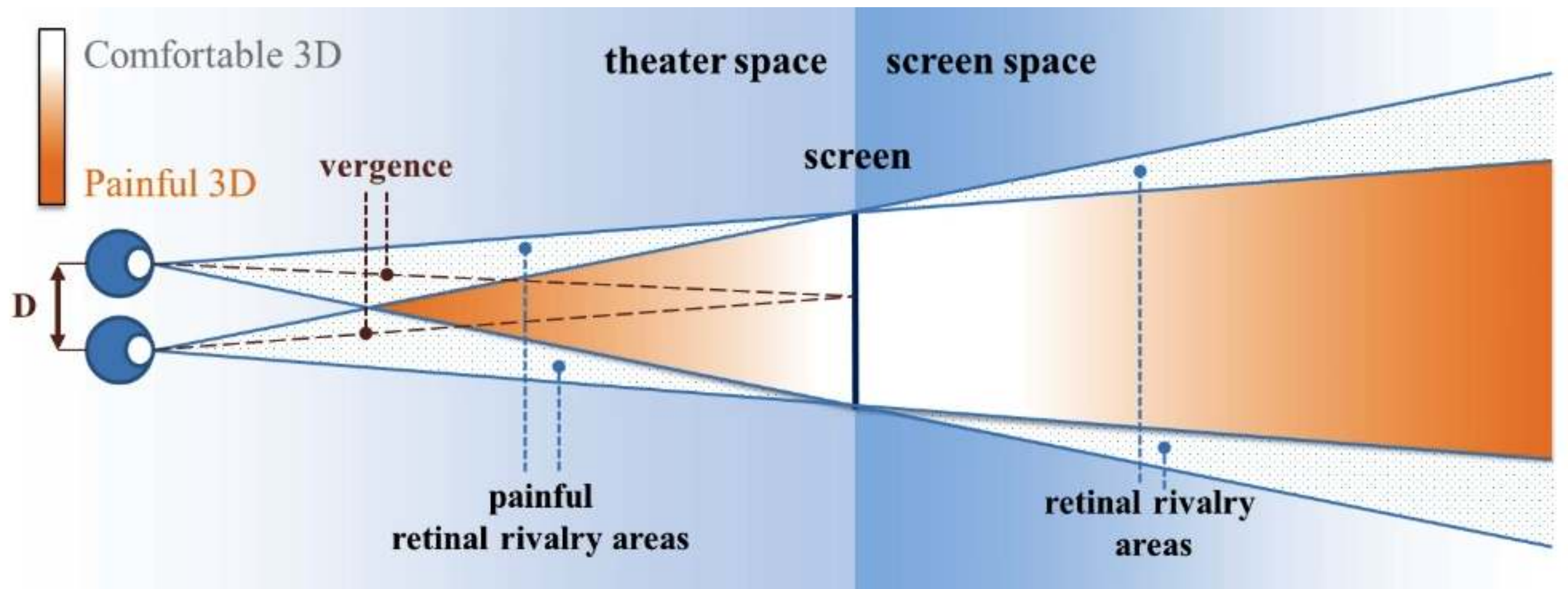
- Introduce disparity mapping operators, which are based on four central aspects of disparity in stereo.
- New technique for applying these disparity mapping operators to stereo 3D footage. The method is based on stereoscopic image warping instead of classical view interpolation.

Four Main Things You Want to Control...

- Disparity Range
- Disparity Sensitivity
- Disparity Gradient
- Disparity Velocity

Stereoscopic Parameters and Operators to Control Them.

Disparity Range

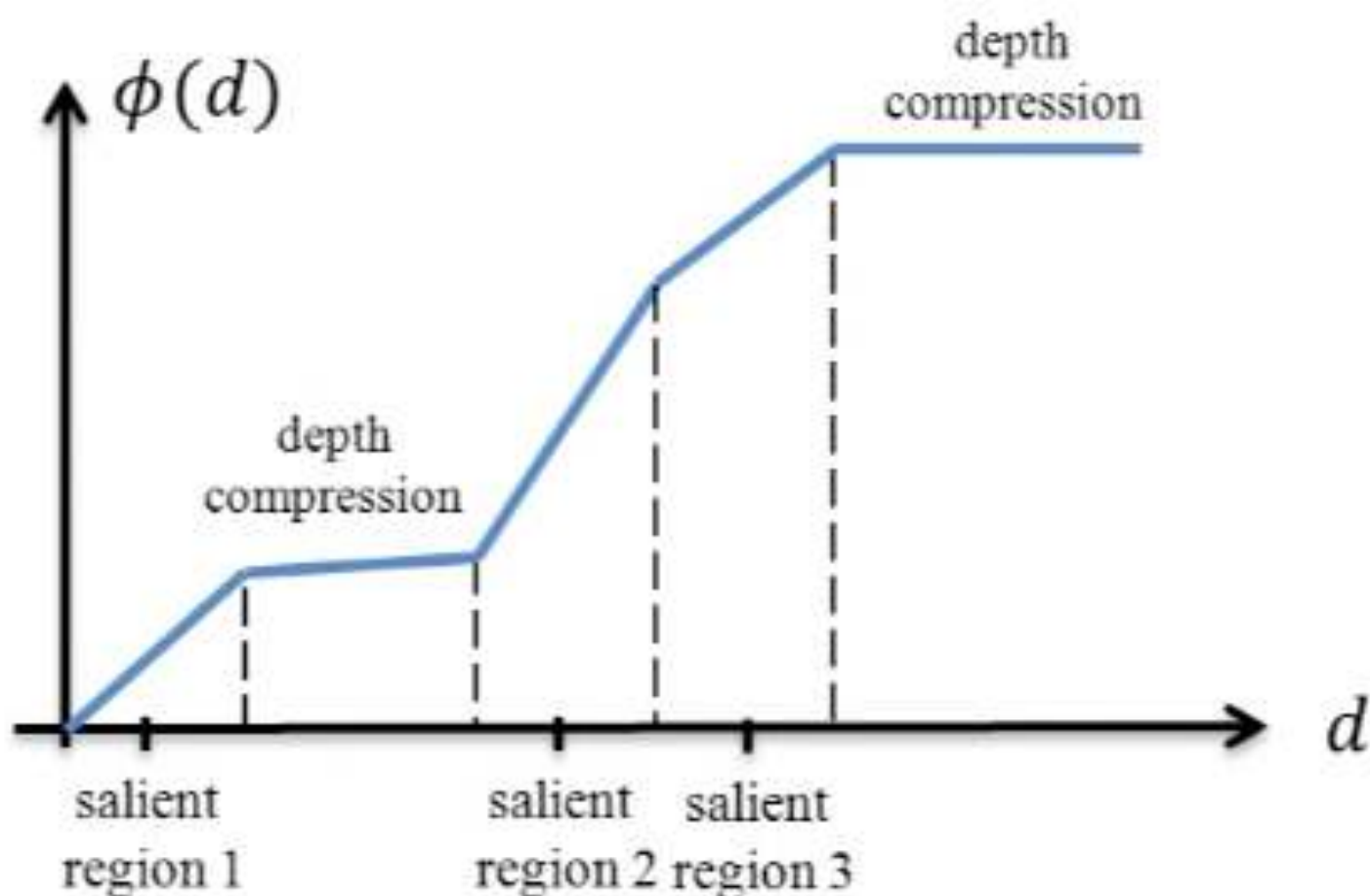


Linear Operator

$$\Phi_l(d) = \frac{d'_{max} - d'_{min}}{d_{max} - d_{min}}(d - d_{min}) + d'_{min}$$

Disparity Sensitivity

Nonlinear Operator



Non-linear Operator

$$\Phi_n(d) = \log(1 + sd)$$

$$\phi_a(d) = \begin{cases} \phi_0(d), & d \in \Omega_0 \\ \dots & \dots \\ \phi_n(d), & d \in \Omega_n \end{cases}.$$

Omega: Target Ranges.

Phi: Corresponding Functions

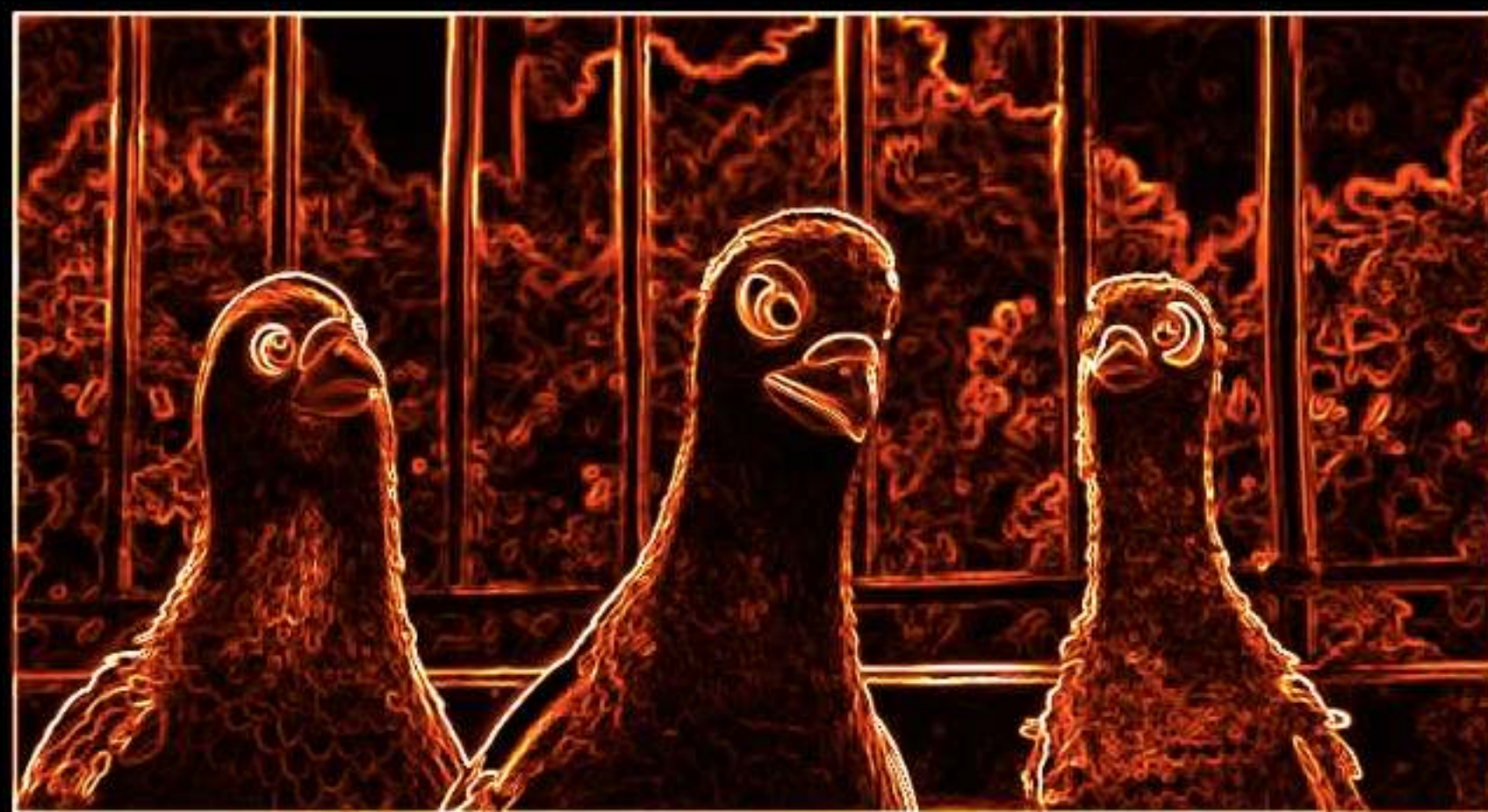
Phi_a: Target Operator

Disparity-based Saliency



Image courtesy of Lang et al.

Local Edge Saliency



© 2010 Disney Enterprises

Image courtesy of Lang et al.

Global Texture Saliency



© 2010 Disney Enterprises

Image courtesy of Lang et al.

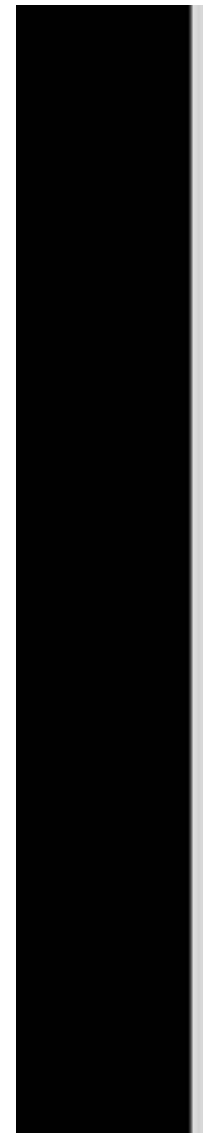
Combined Saliency Map



Image courtesy of Lang et al.

Disparity Gradient

See Burt and Juelsz paper,
“A stereo correspondence algorithm using a
disparity gradient limit”



1. D. J. Poirier and T. Fukukawa, *J. Neurophysiol.* **28**, 737 (1965).
2. H. Korn and D. S. Fuster, *Adv. 38*, 402 (1973).
3. D. S. Fuster and H. Korn, *Science* **179**, 277 (1973).
4. T. Fukukawa and R. T. Farbman, *J. Neurophysiol.* **26**, 349 (1963); Y. Asada, *Zym. J. Physiol.* **13**, 563 (1963).
5. T. Fukukawa, T. Fukukawa, Y. Asada, *J. Gen. Physiol.* **48**, 581 (1965).

6. G. M. Edelman, *MS. 1729 Series 3*.
7. N. J. Burt and R. A. Juelsz, *MS. 1730 Series 3*.
8. H. Korn and D. S. Fuster, *Adv. 38*, 402 (1973).
9. D. S. Fuster and H. Korn, *Science* **179**, 277 (1973).
10. T. Fukukawa and R. T. Farbman, *J. Neurophysiol.* **26**, 349 (1963); Y. Asada, *Zym. J. Physiol.* **13**, 563 (1963).
11. T. Fukukawa, T. Fukukawa, Y. Asada, *J. Gen. Physiol.* **48**, 581 (1965).

19 December 1979

A Disparity Gradient Limit for Binocular Fusion

Abstract. Ever since Passon, it has been commonly assumed that there is an absolute disparity limit for binocular fusion. It is now found that nearby objects modify this disparity limit. This result sheds new light on several enigmatic phenomena in stereograms.

It is generally assumed that a stereoscopically presented object will appear fused and single if its binocular disparity falls within Passon's fisional area (1). When the disparity exceeds this limit, the object will appear double. An object's disparity may be measured relative to the vergence angle of the eyes or relative to another object in the visual field, such as a fixation point. According to the traditional view, the magnitude of this disparity (or disparity difference) is the critical parameter for fusion.

We find, however, that the disparity gradient rather than the disparity magnitude is the limiting factor for fusion when two or more objects occur near one another in the visual field. The disparity gradient is defined between nearby objects as the difference in their disparities divided by their separation in visual angle. Fusion of at least one object fails when this gradient exceeds a critical value (approximately 0.1).

To illustrate an implication of the disparity gradient constraint, consider two objects that are moved toward one another in the visual field, while the distances of the objects from an observer are held constant. The disparity gradient between the objects will increase in inverse proportion to object separation and must eventually exceed the gradient limit for fusion. Thus, each object may appear single when the two are widely separated, but when their angular separation becomes sufficiently small, singleness of one or both will necessarily give way to diplopia. This is true even for objects with very small disparities well within Passon's fisional area.

Dots may appear at different depths, and their half-images may appear fused (single) or diplopic (double). Diplopia occurs when disparities d_L and d_R are large. We find that it also occurs for small d_L and d_R when R_0 is small.

A new type of stereogram was devised for this study, in which the same periodic image is presented to both eyes (Fig. 2B), and depth results from the "wallpaper" effect. Each "wallpaper stereogram" contains many dot pairs of the type shown in Fig. 1 arranged in a regular array. All pairs have the same disparity, d_0 , and orientation, θ_0 . In addition, all pairs within a row have the same separation, R_0 . However, R_0 is increased from row to row as one moves up the stereogram. Thus the disparity gradient, d_0/R_0 , changes systematically over the stereogram.

For an initial experiment, separate stereograms were constructed for each of four angles, θ_0 , and four disparities, d_0 . A range of R_0 was chosen for each stereogram so that fusion was obtained near the top and diplopia near the bottom. Stereograms were drawn on a hard-copy unit (Tektronix 4631) and measured 15 by 20 cm each.

Three subjects viewed the stereograms from 50 cm and reported the number of the row that appeared to fall at the boundary between regions of fusion and diplopia, the row at which fusion and diplopia seemed equally likely to occur.

In a second experiment, the viewing distance was varied in order to extend the range of disparities studied. A set of 15 stereograms differing in disparity but not in orientation ($\theta_0 = 90^\circ$) were viewed from three distances (25, 50, and 100 cm).

Fusion was not always obtained above the reported transition row, and scanning of dots often caused diplopia. Diplopia always occurred below the reported transition row.

The dot separation, R_0 , was determined for each of the rows reported by subjects in three observations of a stereogram. These were averaged to obtain a single estimate of the critical dot separation, \bar{R}_0 , which marked the boundary between fusion and diplopia. Transition values for one observer are

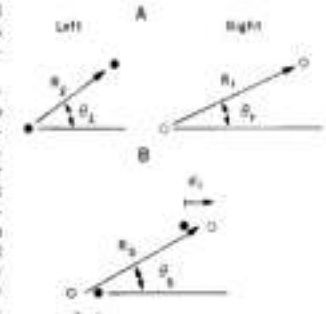


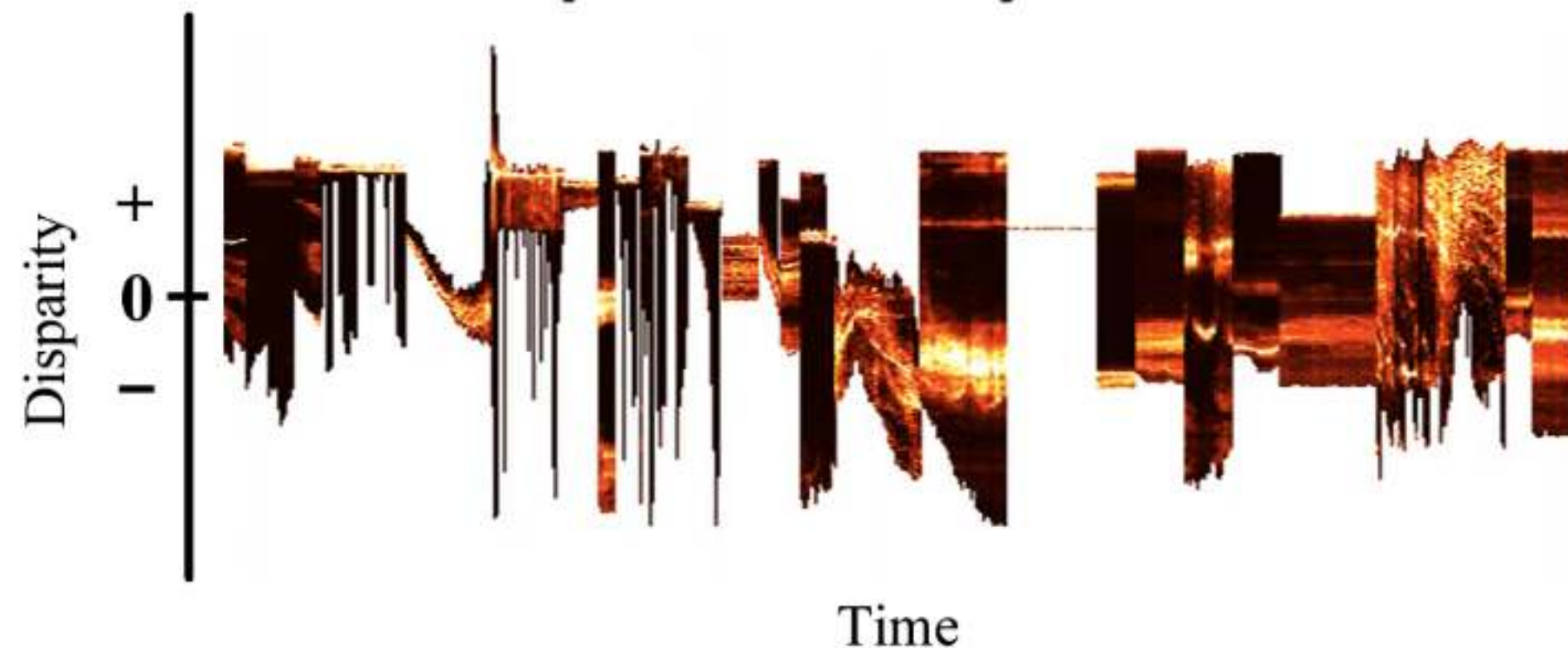
Fig. 1. Geometry of a two-dot stereogram. (A) The half-images shown to each eye and (B) the physical pattern after binocular combination. There is no vertical distance, so $R_0 \sin \theta_0$.

Gradient Domain Operator

$$\begin{aligned}\phi_{\nabla}(\nabla d(\mathbf{x}), S(\mathbf{x})) = & S(\mathbf{x})\phi_l(\nabla d(x)) + \\ & (1 - S(\mathbf{x}))\phi_n(\nabla d(x)).\end{aligned}$$

Disparity Velocity

depth storyboard



Temporal Operator

$$\phi_t(d, t) = \sum_i w_i(t) \phi_i(d),$$

Stereoscopic Warping

Warping

$$O_l \circ w_l = I_l \text{ and } O_r \circ w_r = I_r$$

$$\text{subject to } d(O_l, O_r) = \phi(d(I_l, I_r))$$

sparse stereo
correspondences



sparse stereo
correspondences



Images courtesy of Lang et al.

Stereoscopic Constraint

$$w_l(\mathbf{x}_l) - w_r(\mathbf{x}_r) - \phi(d(\mathbf{x}_l)) = 0,$$

Combined Saliency Map



Image courtesy of Lang et al.

Saliency Constraints

- Distortions: $\frac{\partial w_x}{\partial x} = \frac{\partial w_y}{\partial y} = 1$,
- Bending of edges: $\frac{\partial w_x}{\partial y} = \frac{\partial w_y}{\partial x} = 0$,
- Overlaps: $\frac{\partial w_x}{\partial x} \wedge \frac{\partial w_y}{\partial y} > 0$.

Temporal Constraints

$$\frac{\partial w_x^t}{\partial x}(\mathbf{x}_t) = \frac{\partial w_x^{t-1}}{\partial x}(\mathbf{x}_{t-1}).$$

Solve for Image Warp Enforcing Stereo Constraints

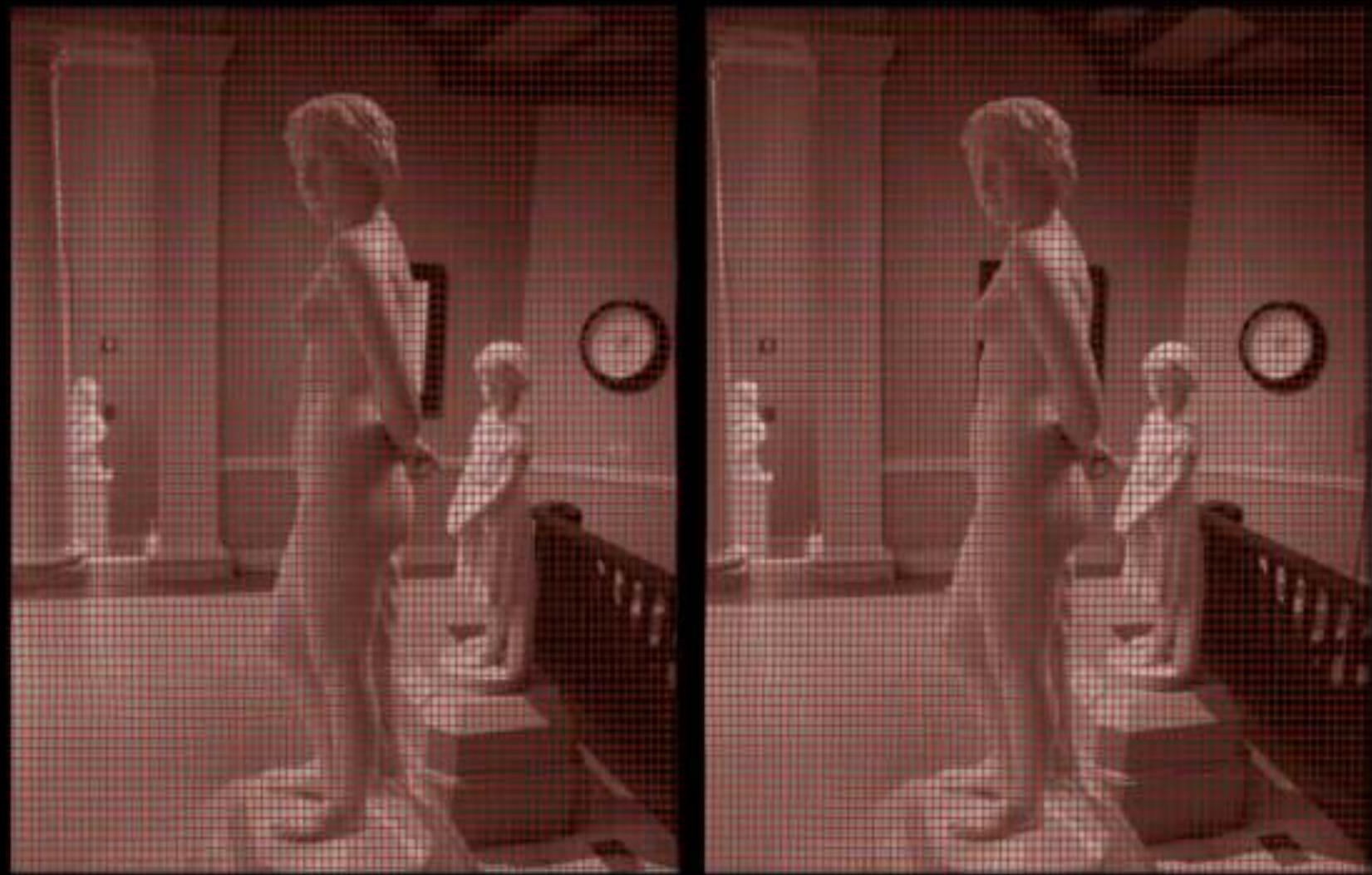


Image courtesy of Lang et al.

Results

Results



solve for
image warp
enforcing stereo consistency